

Acknowledgments

We thank all the family members for participating in this study. We also thank the Commission for Families and Children of Orange County for its support of our clinical work. We appreciate Dr. Takeyori Saheki for useful comments on metabolic decompensation. This study was performed at the Advanced Medical Research Center, Yokohama City University.

Disclosure statement: The authors have no conflict of interest to declare.

References

- Barel O, Shorer Z, Flusser H, Ofir R, Narkis G, Finer G, Shalev H, Nasasra A, Saada A, Birk OS. 2008. Mitochondrial complex III deficiency associated with a homozygous mutation in UQCRCQ. *Am J Hum Genet* 82:1211–1216.
- Benit P, Lebon S, Rustin P. 2009. Respiratory-chain diseases related to complex III deficiency. *Biochim Biophys Acta* 1793:181–185.
- de Lonlay P, Valnot I, Barrientos A, Gorbatyuk M, Tzagoloff A, Taanman JW, Benayoun E, Chretien D, Kadhon N, Lombes A, de Baulny HO, Niaudet P, et al. 2001. A mutant mitochondrial respiratory chain assembly protein causes complex III deficiency in patients with tubulopathy, encephalopathy and liver failure. *Nat Genet* 29:57–60.
- DiMauro S, Schon EA. 2003. Mitochondrial respiratory-chain diseases. *N Engl J Med* 348:2656–2668.
- Fernandez-Vizarra E, Bugiani M, Goffrini P, Carrara F, Farina L, Procopio E, Donati A, Uziel G, Ferrero I, Zeviani M. 2007. Impaired complex III assembly associated with BCS1L gene mutations in isolated mitochondrial encephalopathy. *Hum Mol Genet* 16:1241–1252.
- Ghezzi D, Arzuuffi P, Zordan M, Da Re C, Lamperti C, Benna C, D'Adamo P, Diodato D, Costa R, Mariotti C, Uziel G, Smiderle C, et al. 2011. Mutations in TTC19 cause mitochondrial complex III deficiency and neurological impairment in humans and flies. *Nat Genet* 43:259–263.
- Gudbjartsson DF, Thorvaldsson T, Kong A, Gunnarsson G, Ingolfsdottir A. 2005. Allegro version 2. *Nat Genet* 37:1015–1016.
- Guerois R, Nielsen JE, Serrano L. 2002. Predicting changes in the stability of proteins and protein complexes: a study of more than 1000 mutations. *J Mol Biol* 320:369–387.
- Haut S, Brivet M, Touati G, Rustin P, Lebon S, Garcia-Cazorla A, Saudubray JM, Boutron A, Legrand A, Slama A. 2003. A deletion in the human QP-C gene causes a complex III deficiency resulting in hypoglycaemia and lactic acidosis. *Hum Genet* 113:118–122.
- Hinson JT, Fantin VR, Schonberger J, Breivik N, Siem G, McDonough B, Sharma P, Keogh I, Godinho R, Santos F, Esparza A, Nicolau Y, et al. 2007. Missense mutations in the BCS1L gene as a cause of the Bjornstad syndrome. *N Engl J Med* 356:809–819.
- Iwata S, Lee JW, Okada K, Lee JK, Iwata M, Rasmussen B, Link TA, Ramaswamy S, Jap BK. 1998. Complete structure of the 11-subunit bovine mitochondrial cytochrome bc1 complex. *Science* 281:64–71.
- Khan S, Vihinen M. 2010. Performance of protein stability predictors. *Hum Mutat* 31:675–684.
- Mitsuhashi S, Hatakeyama H, Karahashi M, Koumura T, Nonaka I, Hayashi YK, Noguchi S, Sher RB, Nakagawa Y, Manfredi G, Goto Y, Cox GA, Nishino I. 2011. Muscle choline kinase beta defect causes mitochondrial dysfunction and increased mitophagy. *Hum Mol Genet* 20:3841–3851.
- Schagger H, Pfeiffer K. 2000. Supercomplexes in the respiratory chains of yeast and mammalian mitochondria. *EMBO J* 19:1777–1783.
- Trounce IA, Kim YL, Jun AS, Wallace DC. 1996. Assessment of mitochondrial oxidative phosphorylation in patient muscle biopsies, lymphoblasts, and transmitochondrial cell lines. *Methods Enzymol* 264:484–509.
- Tsurusaki Y, Osaka H, Hamanoue H, Shimbo H, Tsuji M, Doi H, Saitsu H, Matsumoto N, Miyake N. 2011. Rapid detection of a mutation causing X-linked leucoencephalopathy by exome sequencing. *J Med Genet* 48:606–609.
- Visapaa I, Fellman V, Vesa J, Dasvarma A, Hutton JL, Kumar V, Payne GS, Makarow M, Van Coster R, Taylor RW, Turnbull DM, Suomalainen A, et al. 2002. GRACILE syndrome, a lethal metabolic disorder with iron overload, is caused by a point mutation in BCS1L. *Am J Hum Genet* 71:863–876.



Original Article

Exome sequencing in a family with an X-linked lethal malformation syndrome: clinical consequences of hemizygous truncating *OFD1* mutations in male patients

Tsurusaki Y, Kosho T, Hatasaki K, Narumi Y, Wakui K, Fukushima Y, Doi H, Saitsu H, Miyake N, Matsumoto N. Exome sequencing in a family with an X-linked lethal malformation syndrome: clinical consequences of hemizygous truncating *OFD1* mutations in male patients. Clin Genet 2013; 83: 135–144. © John Wiley & Sons A/S. Published by Blackwell Publishing Ltd, 2012

Oral-facial-digital syndrome type 1 (OFD1; OMIM #311200) is an X-linked dominant disorder, caused by heterozygous mutations in the *OFD1* gene and characterized by facial anomalies, abnormalities in oral tissues, digits, brain, and kidney; and male lethality in the first or second trimester pregnancy. We encountered a family with three affected male neonates having an ‘unclassified’ X-linked lethal congenital malformation syndrome. Exome sequencing of entire transcripts of the whole X chromosome has identified a novel splicing mutation (c.2388+1G > C) in intron 17 of *OFD1*, resulting in a premature stop codon at amino acid position 796. The affected males manifested severe multisystem complications in addition to the cardinal features of OFD1 and the carrier female showed only subtle features of OFD1. The present patients and the previously reported male patients from four families (clinical OFD1; Simpson-Golabi-Behmel syndrome, type 2 with an *OFD1* mutation; Joubert syndrome-10 with *OFD1* mutations) would belong to a single syndrome spectrum caused by truncating OFD1 mutations, presenting with craniofacial features (macrocephaly, depressed or broad nasal bridge, and lip abnormalities), postaxial polydactyly, respiratory insufficiency with recurrent respiratory tract infections in survivors, severe mental or developmental retardation, and brain malformations (hypoplasia or agenesis of corpus callosum and/or cerebellar vermis and posterior fossa abnormalities).

Conflict of interest

The authors have no conflict of interest to declare.

**Y Tsurusaki^{a*}, T Kosho^{b*},
K Hatasaki^c, Y Narumi^b,
K Wakui^b, Y Fukushima^b,
H Doi^a, H Saitsu^a, N Miyake^a
and N Matsumoto^a**

^aDepartment of Human Genetics, Yokohama City Graduate School of Medicine, Yokohama, Japan,

^bDepartment of Medical Genetics, Shinshu University School of Medicine, Matsumoto, Japan, and ^cDepartment of Pediatrics, Toyama Prefectural Central Hospital, Toyama, Japan

*These authors contributed equally to this work.

Key words: exome sequencing – OFD1 – *OFD1* gene – splicing mutation – X-linked congenital malformation syndrome

Corresponding authors: Tomoki Kosho, MD, Department of Medical Genetics, Shinshu University School of Medicine, 3-1-1 Asahi, Matsumoto, Nagano 390-8621, Japan.

Tel.: +81 263 37 2618;

fax: +81 263 37 2619;

e-mail: ktomoki@shinshu-u.ac.jp

and

Naomichi Matsumoto, MD, PhD, Department of Human Genetics, Yokohama City Graduate School of Medicine, 3-9 Fukuura, Kanazawa-ku, Yokohama 236-0004, Japan.

Tel.: +81 45 787 260;

fax: +81 45 786 5219;

e-mail: naomat@yokohama-cu.ac.jp

Received 14 January 2012, revised and accepted for publication 26 March 2012

Oral-facial-digital syndrome type 1 (OFD1; OMIM #311200), originally described by Papillon-Leage and Psaume (1) and further delineated by Gorlin and Psaume (2), is an X-linked dominant developmental disorder with an estimated prevalence of 1:50,000, caused by mutations in the *OFD1* gene (OMIM #300170) (3–5). The disorder is characterized by facial anomalies and abnormalities in oral tissues, digits, brain and kidney (5). Almost all affected individuals with OFD1 are female, with highly variable expression, possibly resulting from random X inactivation (6). Affected males are generally lost in the first or second trimester of pregnancy (4). To date, only one liveborn male case with clinically definite OFD1 and a normal karyotype has been reported; the patient was born at 34 weeks of gestation and died 21 h after birth due to heart failure (7). In this report, we describe a family with three affected male neonates having an ‘unclassified’ X-linked lethal congenital malformation syndrome. Exome sequencing of entire transcripts of the whole X chromosome has successfully identified a causative splicing mutation in *OFD1*.

Subjects and methods

Clinical report

II-2, a 22-year-old woman, was referred to our clinic for genetic counseling (Fig. 1). Her deceased brother (II-4) had severe multiple congenital abnormalities. She had two sons (III-1 and III-5) with similar congenital abnormalities and a healthy boy (III-3) as well as two miscarriages (III-2, artificial; III-4, spontaneous). During genetic counseling and molecular investigations, she had another healthy boy (III-5). After identification of a heterozygous *OFD1* mutation, she was examined for features of OFD1. Only a few accessory frenulae and irregular teeth with no facial anomalies or tongue abnormalities were observed (Fig. 2a–e). A radiograph of her hands showed no abnormalities (Fig. 2f) and an abdominal ultrasonography detected no cysts in the kidneys, liver, or pancreas (data not shown). I-2, allegedly, had no apparent malformations or complications including renal diseases.

II-4 was born by caesarean section because of placental abruption at 33 weeks of gestation. Pregnancy was complicated by polyhydramnios. Apgar score was 3 at 1 min. His birth weight was 2056 g (+0 SD), length was 45.0 cm (+0.5 SD), and occipitofrontal circumference (OFC) was 34.0 cm (+2.0 SD). He manifested severe respiratory insufficiency and was transferred to a neonatal intensive care unit (NICU). His craniofacial features included a prominent forehead, a large fontanelle (5 × 5 cm), a low posterior hair-line, microphthalmia, hypertelorism, short palpebral fissures, depressed nasal bridge, low-set ears, a small cleft lip and a soft cleft palate, narrowing of the tip of the tongue, and a hypoplastic gum (Fig. 2g). Additional physical features included redundant neck skin, postaxial polydactyly of the left hand (Fig. 2h), wide halluces (Fig. 2i), micropenis, and left cryptorchidism.

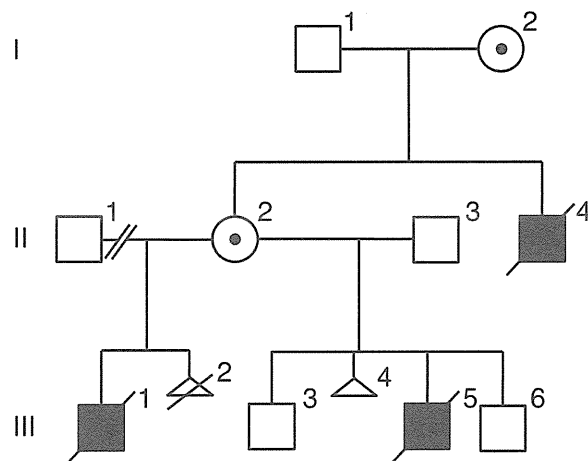


Fig. 1. Familial pedigree.

Ultrasonography revealed hypoplastic gyri, an atrial septal defect, and patent ductus arteriosus. Ophthalmological examination detected microcornea and retinal detachment. Intubation was impossible because of laryngeal anomalies and the patient died 11 h after birth. Additional autopsy findings included partial atelectasis and bilateral hydronephrosis.

III-1 was delivered by emergency caesarean section at 39 weeks of gestation. Pregnancy was complicated by polyhydramnios and intrauterine growth retardation, with moderate macrocephaly. His birth weight was 3064 g (+0.1 SD). He was admitted to a NICU because of respiratory insufficiency, and received mechanical ventilation. His craniofacial features included microphthalmia, hypertelorism, short palpebral fissures, epicanthus, low-set ears, and a cleft lip and palate. Additional physical features included bilateral polydactyly of hands (postaxial) and feet (preaxial), and an ectopic urethral opening. Ultrasonography revealed hydrocephalus, agenesis of the corpus callosum and cerebellar vermis, and a complete atrioventricular septal defect. Ophthalmological examination detected persistent pupillary membrane and optic disc coloboma. G-banded chromosomes were normal (46,XY). The patient died at age 14 days due to heart failure.

III-5 was delivered by caesarean section at 32 weeks of gestation. Pregnancy was complicated by polyhydramnios, intrauterine growth retardation, and congenital heart defects. His birth weight was 1704 g (–0.2 SD), length was 40.0 cm (–0.8 SD), and OFC was 33.3 cm (+2.0 SD). He was admitted to a NICU because of respiratory insufficiency, and received mechanical ventilation. His craniofacial features included a prominent forehead, hypertelorism, dysplastic ears, a small cleft lip, and a soft cleft palate (Fig. 2j,k). Ultrasonography revealed hydrocephalus with Dandy-Walker malformation and hypoplastic left heart syndrome. G-banded chromosomes were normal (46,XY). The patient died 1 day after birth. Additional autopsy findings included agenesis of the cerebellar vermis (Fig. 2l), enlargement of the fourth ventricle and aqueduct, anomalous positioning of the esophagus, mild

Exome sequencing in a family with an X-linked lethal malformation syndrome

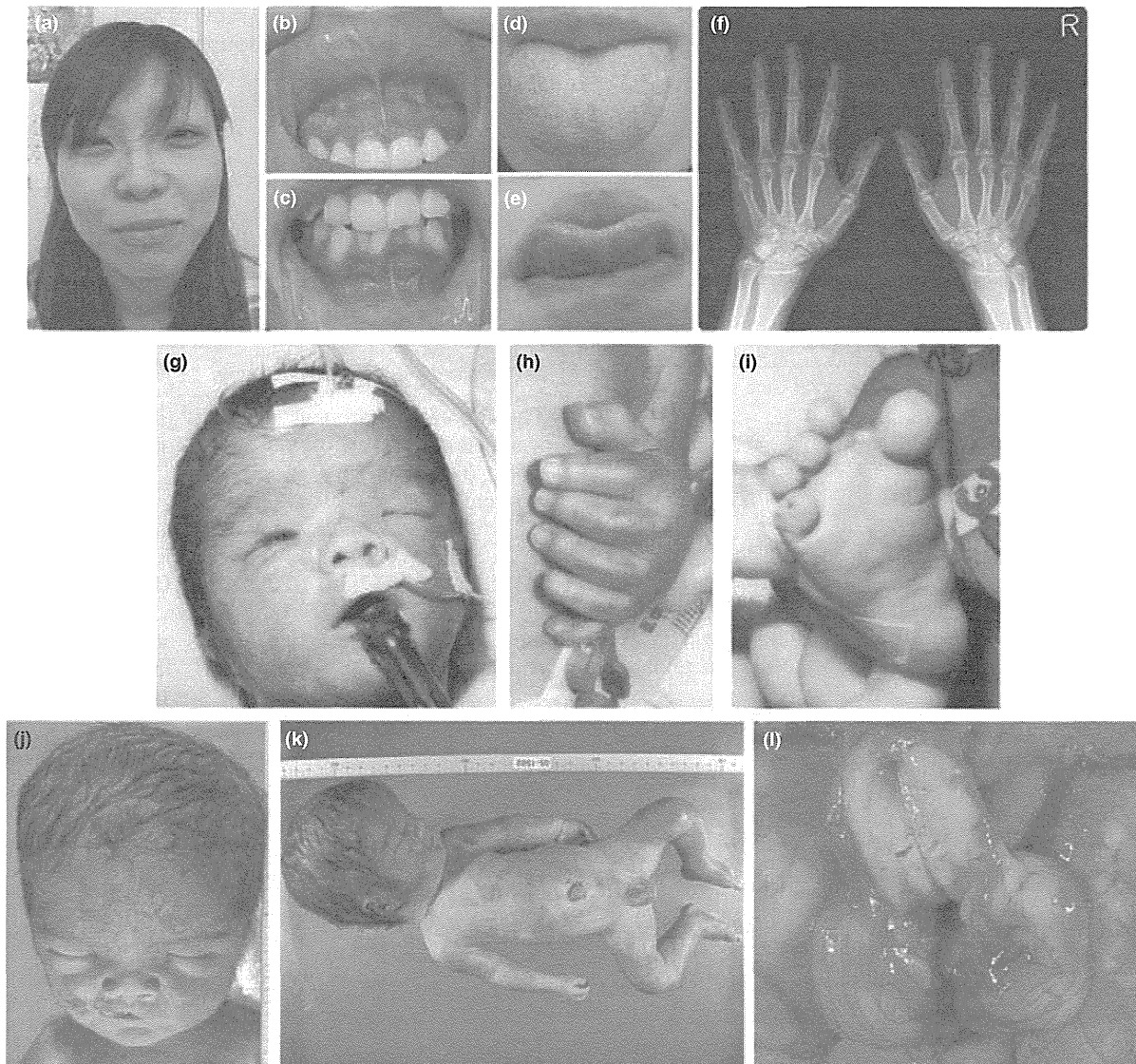


Fig. 2. Clinical photographs of II-2 (a–f), II-4 (g–i), and III-5 (j–l).

pulmonary congestion, and insufficient lobulation of the right lung.

The three affected male neonates, having strikingly similar clinical manifestations (Table 1), are considered to have had a congenital malformation syndrome with X-linked inheritance. Array-CGH analysis using 4200 BAC clones identified no pathologic genomic copy number abnormalities. Direct sequencing of *MID*, performed because of a partial similarity to these neonates' syndrome to X-linked Opitz-G/BBB syndrome (OMIM #300000) (8), revealed no mutation.

Library preparation

Genomic DNA for II-2, II-3, III-3, and III-6 was extracted from peripheral blood using the Genra PureGene Blood Kit (QIAGEN, Hilden, Germany), and genomic DNA for III-5 was extracted from the preserved dried umbilical cord using the DNeasy Blood

& Tissue Kit (QIAGEN). Three micrograms of high-quality (absorbance at 260 nm/absorbance at 280 nm: 1.8–2.0) genomic DNA from II-2 was fragmented using the Covaris model S2 system (Covaris, Woburn, MA). The target peak size was 150 bp. After the size of sheared DNA was checked using an Agilent 2100 Bioanalyzer (Agilent Technologies, Santa Clara, CA), adapter sequences were ligated to the ends of DNA fragments, and amplified according to the manufacturer's protocol (Agilent Technologies).

Exome capture and next-generation sequencing

Library DNA was hybridized for 24 h at 65°C using the SureSelect Human X Chromosome Demo Kit (Agilent Technologies). Captured DNA was diluted to a concentration of 8 pM and sequenced on a Genome Analyzer IIx (Illumina, San Diego, CA) with 76-bp paired-end reads. We used only one of the eight lanes in the flow

Table 1. Variant priority scheme after exome sequencing^a

| | NEXTGENE | II-2 | MAQ (SEATTLESEQ) |
|--|----------|------|---------------------|
| Total variants called | 22,176 | — | 58,081 |
| Chr X | 3441 | — | 4383 |
| Unknown SNP variants (dbSNP131, 1000 genomes) | 910 | — | 882 |
| Overlap of NEXTGENE and MAQ | — | 169 | — |
| NS/SS | — | 17 | — |
| Except for variants at segmental duplications | — | 15 | — |

NS, non-synonymous; SNP, single-nucleotide polymorphism; SS, splice site (± 2).

^aMAQ was annotated with SEATTLESEQ ANNOTATION. The annotation includes gene names, dbSNP rs ID, and SNP functions (e.g. missense), protein positions and amino acid changes.

cell for II-2 (Illumina). Image analyses and base calling were performed using sequence control software real-time analysis and OFFLINE BASECALLER software v1.8.0 (Illumina). Reads were aligned to the human reference genome (UCSC hg19, NCBI build 37.1).

Mapping strategy and variant annotation

The quality-controlled (Path Filter) reads were mapped to the human reference genome (UCSC hg19, NCBI build 37.1), using mapping and assembly with quality (MAQ) and NEXTGENE software v2.0 (SoftGenetics, State College, PA). Single-nucleotide polymorphisms in MAQ-passed reads were annotated using the SEATTLESEQ ANNOTATION website (<http://gvs.gs.washington.edu/SeattleSeqAnnotation/>).

Priority scheme and capillary sequencing

Called variants found by each informatics method were filtered in terms of location on chromosome X, unregistered variants (excluding registered dbSNP131 and 1000 Genomes), overlapping variants called in common by NEXTGENE and MAQ, and non-synonymous changes and splice-site mutations (± 2 bp from exon-intron junctions) (Table 1). The variants were confirmed as true positives by Sanger sequencing of polymerase chain reaction (PCR) products amplified using genomic DNA as a template, except for variants within genes at segmental duplications. Sanger sequencing was performed on an ABI3500xl or ABI3100 autosequencer (Life Technologies, Carlsbad, CA). Sequencing data were analyzed using SEQUENCHER software (Gene Codes Corporation, Ann Arbor, MI).

Reverse transcription-PCR

Total RNA was isolated from EBV-transformed lymphoblastoid cell line (EBV-LCL) derived from II-2 and healthy control subjects using the RNeasy Plus Mini

Kit (QIAGEN). Five micrograms of total cellular RNA was used for reverse transcription with the Super Script III First-Strand Synthesis System (Life Technologies). Two microliters of synthesized complementary DNA was used for PCR with the following primers: ex17-F (5'-CTACCATCACCCACTGAGTC-3') and ex19-R (5'-TGAGACATATCCCCGGCAG-3'). Amplified PCR products were electrophoresed in agarose gels, purified from gels using the QIAquick Gel Extraction Kit (QIAGEN), cloned into pCR4-TOPO vector (Life Technologies) and sequenced.

X-chromosome inactivation assay

The human androgen receptor (HUMARA) assay was performed as previously reported (9). Genomic DNA of II-2 was digested at 37°C for 18 h with two methylation-sensitive enzymes, *Hpa*II and *Hha*I. PCR was performed using digested and undigested DNA with HUMARA primers (FAM-labeled ARF: 5'-TCCAGAATCTGTTCAGAGCGTGC-3'; ARr: 5'-CTCTACGATGGGCTTGGGGAGAAC-3'). DNA fragment analysis was performed on an ABI3130xl autosequencer (Life Technologies). Fragment data were analyzed with GENEMAPPERT SOFTWARE version 4.1 (Life Technologies).

Results

Exome sequencing

Because this disorder was assumed to be an 'X-linked recessive' disorder based on the initial pedigree information, we focused on the X chromosome. Approximately 4.5 Gb of sequence data were generated, 87.3% of which was mapped to the human reference genome (UCSC hg19, NCBI build 37.1). MAQ was able to align 53,242,972 reads to the whole genome.

Two informatics methods identified 17 potential pathogenic changes (15 missense mutations, 1 nonsense mutation, and 1 splice-site mutation) (Table 1). The nonsense mutation was a false positive and all 13 missense mutations were inconsistent with the phenotype (no co-segregation). The mutation c.2388+1G>C was identified at the splice-acceptor site of intron 17 in *OFD1*, heterozygously in II-2, and hemizygotously in III-5, but was absent in II-3, III-3, and III-6 (Fig. 3a) as well as 93 normal female controls (0/186 alleles).

RT-PCR, direct sequencing

To examine the mutational effects of c.2388+1G>C, reverse transcriptase-polymerase chain reaction (RT-PCR) was performed. Only a 239-bp PCR product (wild-type allele) was observed in healthy control individuals (Fig. 3b). By contrast, a longer 1364-bp product was detected in II-2. Sequencing of the 1364-bp product revealed that a 1125-bp sequence of intron 17 was retained, producing a premature stop codon at amino acid position 796 (Fig. 3b). These data indicate

Exome sequencing in a family with an X-linked lethal malformation syndrome

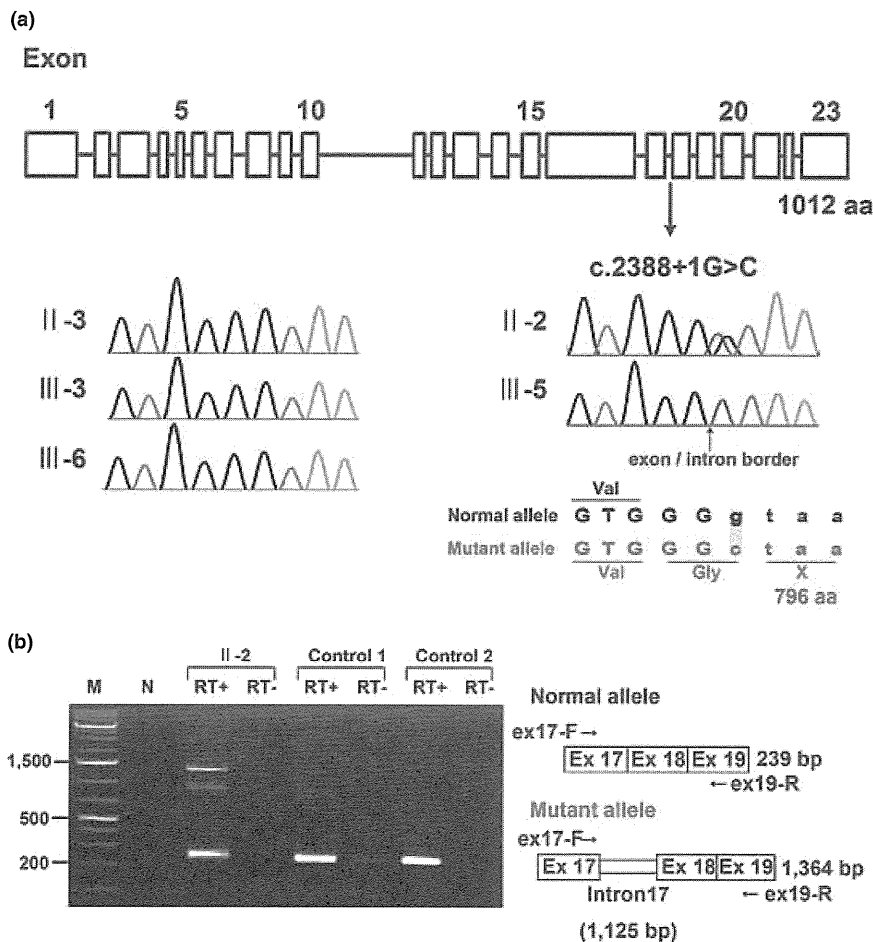


Fig. 3. (a) Gene structure of *OFDI* with the mutation (c.2388+1G>C) (upper). Electropherograms of the family members. Wild-type sequences are seen in II-3, III-3 and III-6. Heterozygous and hemizygous mutations are observed in II-2 and III-5, respectively. (b) Reverse transcriptase-polymerase chain reaction analysis showing both 239-bp and 1364-bp products in II-2, and only 239-bp products in two normal female controls. The 239-bp product is normal and the 1364-bp product is aberrant.

that the c.2388+1G>C mutation in *OFDI* is most likely the causal mutation in this family.

X-chromosome inactivation assay

X-chromosome inactivation patterns was random patterns in II-2 available for this study (ratio > 38:62).

Discussion

Exome sequencing detected a single-base substitution (c.2388+1G>C) in *OFDI*, resulting in an error in splicing of intron 17 and a premature stop codon at amino acid position 796, in an affected male (III-5) and a carrier female (II-2) in this family with an 'unclassified' X-linked lethal congenital malformation syndrome. II-4 and III-1, who had strikingly similar clinical manifestations to III-5, are likely to have had the same *OFDI* mutation as III-5, although their DNA was not available. Through reassessment of clinical features of the family, the three affected males shared facial, oral, and digital malformations characteristic of OFD1 (4). Additionally, they exhibited more severe

complications in various systems including congenital heart defects, genitourinary malformations, and ophthalmological abnormalities. II-2 was also found to have subtle features of OFD1 (accessory frenulae and irregular teeth). Thus, we have concluded that the 'unclassified' X-linked lethal congenital malformation syndrome in this family was clinically compatible with OFD1.

An *OFDI* mutation (c.2123_2126dupAAGA in exon 16, p.Asn711Lysfs*3) was also detected in a family with an X-linked recessive mental retardation syndrome (10). Nine affected males had macrocephaly and severe mental or developmental retardation, and suffered from recurrent respiratory tract infections leading to early death in eight. Only an 11-year-old boy survived with severe mental retardation (IQ 20), obesity, and brachydactyly. His younger brother had postaxial polydactyly. No cognitive, oral, facial, digital, or renal abnormalities were detected in heterozygous carrier females in that family. The patients were later classified into an infantile lethal variant of Simpson-Golabi-Behmel syndrome (type 2) (SGBS2, OMIM #300209), which had consisted of only one family,

genetically mapped to Xp22, including four maternally related affected males with hydrops at birth, craniofacial anomalies (macrocephaly, low-set posteriorly angulated ears, hypertelorism, short and broad nose with anteverted nares, large mouth with thin upper vermilion border, prominent philtrum, high-arched or cleft palate, and short neck), redundant skin, hypoplastic nails, skeletal defects involving upper and lower limbs, gastrointestinal and genitourinary anomalies, hypotonia and neurological impairment, and early death within the first 8 weeks (11, 12). Other *OFD1* mutations were detected in two families with Joubert syndrome-10 (JBTS10, OMIM #213300) (13). A mutation (c.2844_2850delAGACAAA in exon 21, p.Lys948Asnfs*9) in a family with eight affected males caused severe mental or developmental retardation and recurrent infections in all; postaxial polydactyly in five, retinitis pigmentosa in three, and a molar tooth sign on brain magnetic resonance imaging (MRI) in two. No heterozygous carrier females had any symptoms similar to those in the affected males. Another mutation (c.2767delG in exon 21, p.Glu923Lysfs*4) was found *de novo* in a 12-year-old male patient with severe mental retardation, macrocephaly, obesity, postaxial polydactyly, and a molar tooth sign on brain MRI (13).

To discuss whether these male patients with hemizygous truncating *OFD1* mutations would have different conditions (*OFD1*, *SGBS2*, or *JBTS10*) or belong to the same syndrome spectrum, we have created a comprehensive list of clinical manifestations in all of them (Table 2) (7, 10, 13). Macrocephaly, polydactyly (postaxial), respiratory insufficiency with recurrent respiratory tract infections in survivors, and severe mental or developmental retardation were shared by all the families (7, 10, 13). Nasal bridge features (depressed or broad) and lip abnormalities (cleft lip, pseudocleft lip, full lips, and prominent philtrum) were shared by the families with *OFD1* and *JBTS10* (7, 13). Brain malformations including hypoplasia or agenesis of corpus callosum, hypoplasia or agenesis cerebellar vermis as well as posterior fossa abnormalities (large, occipital encephalocele) were also shared by the families with *OFD1* and *JBTS10* (7, 13). III-5 in the present family was described to have Dandy-Walker malformation on brain ultrasonography. Three patients with *JBTS10* were described to have a molar tooth sign on brain MRI, which is the characteristic neuroradiological hallmark of Joubert syndrome (13). Dandy-Walker malformation, typically consisting of agenesis or hypoplasia of cerebellar vermis, a cystic dilatation of the fourth ventricle, and an enlarged posterior fossa with a high position of the tentorium, is usually distinguishable from Joubert syndrome, characterized anatomically by agenesis or hypoplasia of cerebellar vermis and enlargement of the superior cerebellar peduncles and deep interpeduncular fossa resulting from a lack of normal decussation of superior cerebellar peduncular fiber tracts, leading to the characteristic 'molar tooth' appearance on transverse computed tomography and MRI of the mid-brain (14); and clinically by hypotonia, developmental

retardation, abnormal respiratory patterns, and oculomotor apraxia (15). However, Joubert syndrome could be present in association with Dandy-Walker malformation (15); and in such a case, Dandy-Walker malformation was reported to have initially masked the molar tooth sign because of a cystic dilatation of the fourth ventricle (16). Some authors state that the presence of the molar tooth sign does not, in itself, allow a diagnosis, Joubert syndrome, to be made; but that clinical evidence of the syndrome including hypotonia and developmental retardation accompanied by either abnormal breathing or abnormal eye movements should be present (14, 17). Typical respiratory abnormalities in Joubert syndrome, represented by short alternate episodes of apnea and hyperpnea or episodic hyperpnea alone (18), were not described in the patients with *JBTS10*, with only one presenting with stridor and intermittent cyanosis soon after birth (13). Abnormal eye movements including oculomotor apraxia were not mentioned in those with *JBTS10* (13). In view of these evidences, it is reasonable to consider that the male patients with *OFD1* mutations, identified to date, would belong to a clinical continuum with wide intra- and inter-familial phenotypic variations of a single disorder.

A review by Macca and Franco (4) summarized all reported mutations in *OFD1* patients. In total, 99 different mutations (7 genomic deletions and 92 point mutations) were identified, including 67 frameshift mutations (58%), 14 missense mutations (12%), 14 splice-site mutations (12%), 13 nonsense mutations (11%), and an in-frame deletion. Point mutations occur only in the first 17 exons (*OFD1* consists of 23 exons). A significant genotype-phenotype correlation between high-arched/cleft palate and missense and splice-site mutations has been identified (19). In addition, cystic kidney is more frequently associated with mutations in exons 9 and 12 (19). Quantitative PCR analysis of *OFD1* mRNA levels in EBV-LCLs from two families with *JBTS10* showed that 30% and 58% of *OFD1* expression remained, suggesting that the mutant mRNA would be subject to nonsense-mediated decay and that the phenotypic variability observed for *OFD1* mutations would be caused by changes in activity of remaining truncated *OFD1* protein (13). To date, premature stop codons at 713 in exon 16 (19), 796 in exon 17 (this report), 926 in exon 21 (13), and 956 in exon 21 (13) are associated with survival in males with hemizygous truncating *OFD1* mutations and no or subtle clinical manifestations in females with heterozygous *OFD1* mutations. Heterozygous truncating *OFD1* mutations preserving normal exons 1-16 have been reported in only two families with typical female *OFD1* patients: a single-base deletion (c.2349delC in exon 17, p.Ileu784Serfs*85) (20) and a deletion of complete exon 17 (21). Mutations producing longer truncated protein (~ exon 17) might cause a milder form of the disorder that could not be detected in typical female *OFD1* patients, but could be detected in male patients with multiple congenital anomalies and probable lethality in childhood.

Table 2. Clinical features of male patients with *OFD1* mutations

| Patient | Family 1 (present family) | | | Family 2 ^b | Family 3 ^c | | | | Family 4 ^d (W07-713) | | | Family 5 ^d (UW87) | Carrier |
|---|---------------------------|-----------|-----------|-----------------------|-----------------------|-----------|-----------|------------|---------------------------------|---------------------|------------|------------------------------|----------------------------|
| | II-4 | III-1 | III-5 | 1 | IV-1 | IV-3 | IV-11 | 6 Patients | III-9 | IV-10 | 6 Patients | | 19 Females |
| Age | 0d/D | 14d/D | 1d/D | | 11 y | 18 m/D | 3 y/D | D | 34 y | 3.5 y | D (3) | | |
| Birth weight (g) (gestational age) | 2056 (33) | 3064 (39) | 1704 (32) | | 3850 (40) | 4120 (38) | 1915 (35) | | | 3050 (Te) | | 4090 (41) | |
| Macrocephaly (>1.5 SD) | + | | + | | + | + | + | Some | | | | + | |
| Obesity | | | | | + | | | | - | - | - | + | |
| Craniofacial (87.3% ^a) | | | | | | | | | - | - | - | | |
| Facial anomalies (69.1% ^a) | | | | | | | | | | | | | |
| Prominent forehead | + | | + | | | | | | | | | | |
| Redundant neck skin | + | | | | | | | | | | | + | |
| Hypertelorism | + | + | + | + | | | | | | | | | |
| Epicanthus | | + | | | | | | | | | | | |
| Short palpebral fissures | + | + | | | | | | | | | | | |
| Nasal bridge features | Dep | | Dep | | | | | | Br | Br | | Dep | |
| Low-set ears | + | + | | | + | | | | + | + | | | |
| Lip abnormalities (32.6% ^a) | PCL | CL | PCL | PCL | | | | | F _L , PP | F _L , PP | | PCL | PCL (1) |
| Oral | | | | | | | | | | | | | |
| Palatal abnormalities (49.6% ^a) | CSP | CP | CSP | CSP | HP | | | | | | | | |
| Accessory frenulae (63.7% ^a) | | | | | | | | | | | | | |
| Tongue abnormalities (84.1% ^a) | Nar | | | | | | | | | | | MG | + (4) Lob (3) lr (1) |
| Teeth abnormalities (43.3% ^a) | | | | | | | | | | | | | |
| Skeletal | | | | | | | | | | | | | |
| Short fingers/brachydactyly | | | | | + | | + | | | - | | + | |
| Postaxial polydactyly (3.7% ^a) | LtH | BiH | | BIHRtBLT | | RtH | | | | BiHF | BiHF (4) | BiHLtF | |
| Preaxial polydactyly (19.3% ^a) | BiBrHx | BiF | | BiBHx | BiBrT | | | | | | | | |
| Respiratory | | | | | | | | | | | | | |
| Laryngeal anomalies | + | | | | | | | | | | | | |
| Respiratory insufficiency | + | + | | | | + | | | | + | | | |
| Recurrent infections | | | | | + | + | + | + | + | + | + | + | |
| Cardiovascular | | | | | | | | | | | | | |
| Congenital heart defects | ASD, PDA | AVSD | HLHS | AVSD | | | | | | | | | |
| Genitourinary | | | | | | | | | | | | | |
| Cystic kidney | - | | - | | - | - | | | - | - | - | - | |
| Urinary tract abnormalities | HU | EUO | | | | | | | | | | | |
| Genital abnormalities | MP, C | | | | | | | | | | | | |
| Gastrointestinal | | | | | | | | | | | | | |
| Esophageal abnormalities | | | + | | | | | | | | | | |
| Ophthalmological | | | | | | | | | | | | | |
| Microphthalmia/microcornea | + | | | | | | | | | | | | |
| Persistent papillary membrane | | + | | | | | | | | | | | |

Exome sequencing in a family with an X-linked lethal malformation syndrome

Table 2. Continued

| Patient | Family 1 (present family) | | | Family 2 ^b | Family 3 ^c | | | | Family 4 ^d (W07-713) | | | Family 5 ^d (UW87) | Carrier |
|--|---------------------------|-------|-------|-----------------------|-----------------------|------|-------|------------|---------------------------------|-------|------------|------------------------------|------------|
| | II-4 | III-1 | III-5 | 1 | IV-1 | IV-3 | IV-11 | 6 Patients | III-9 | IV-10 | 6 Patients | | 19 Females |
| Optic disc coloboma | | + | | | | | | | | | | | |
| Optic nerve atrophy | | | | | | | | | | | | | + |
| Retinal detachment | + | | | | | | | | | | | | |
| Retinitis pigmentosa | | | | | | | | | + | + | + | (1) | - |
| Central nervous system (48.4% ^a) | | | | | | | | | | | | | |
| Hydrocephalus | | + | + | + | - | - | + | | | | | | |
| Gyrus abnormalities | Hp | | | PM | - | - | - | | | | | | |
| Corpus callosum abnormalities | | Ag | | Ag | - | - | - | | | | | | Hp |
| Cerebellar vermis abnormalities | | Ag | Ag | | - | - | - | | Hp | Hp | | | |
| Thick superior cerebellar peduncles | | | | | - | - | - | | + | + | | | |
| Molar tooth sign | | | | | - | - | - | | + | + | | | + |
| Dandy-Walker malformation | | | + | | - | - | - | | | | | | |
| Posterior fossa abnormalities | | | | L | - | - | - | | | L | | | EC |
| Developmental/mental retardation | | | | | S | S | + | S | S | S | + | (All) | S |

+, present; -, absent; blank, data not available; Ag, agenesis; ASD, atrial septal defect; AVSD, atrioventricular septal defect; BHx, bifid halluces; Bi, bilateral; BLT, bifid little toe; Br, broad; C, cryptorchidism; CL, cleft lip; CP, cleft palate; CSP, cleft soft palate; d, days; D, death; Dep, depressed; EC, encephalocele; EUO, ectopic urethral opening; F, foot/feet; FL, full lips; H, hand(s); HF, hands and feet; HLHS, hypoplastic left heart; Hp, hypoplasia; HP, high palate; HU, hydroureter; Hx, halluces; Ir, irregular; L, large; Lob, lobulated; Lt, left; m, months; MG, midline groove; MP, micropenis; Nar, narrowing of the tip of the tongue; PCL, pseudocleft of the upper lip; PDA, patent ductus arteriosus; PM, polymicrogyria; PP, prominent philtrum; Rt, right; S, severe; Te, term; T, thumbs; y, years.

^aFrom Macca and Franco (4).

^bFrom Goodship et al. (7).

^cFrom Budny et al. (10).

^dFrom Coene et al. (13).

Exome sequencing in a family with an X-linked lethal malformation syndrome

High-throughput, next-generation sequencing (NGS) has had a tremendous impact on human genetic research (22). Moreover, techniques enabling enrichment of selected regions enable us to use NGS efficiently and to identify the causative genes for a reasonable number of genetic disorders as well as susceptibility genes for complex diseases and health-related traits (23). In particular, X-linked disorders are good candidates for exome sequencing. We recently identified a nonsense mutation in *MCT8* causing X-linked leukoencephalopathy in a family from only two affected male samples (24). We have also identified two possible but inconclusive missense variants (*LICAM* and *TMEM187*) in a family with an atypical X-linked leukodystrophy from only two affected male samples (25). In this study, exome sequencing accompanied by appropriate bioinformatics techniques and a co-segregation evaluation successfully revealed a disease-causing mutation in *OFDI*, which could not have been assumed to be a candidate based on the clinical manifestations of the affected male patients. Unbiased rapid screening through these technologies is a powerful method for the detection of mutations in unexpected causative genes in undiagnosed patients with multiple congenital malformations.

In conclusion, we have identified a causative splicing mutation in *OFDI*, through exome sequencing, in a family with three males having an 'unclassified' X-linked lethal congenital malformation syndrome. The affected males manifested severe multisystem complications in addition to the cardinal features of OFDI and the carrier female showed only subtle features of OFDI. The present patients, as well as the previously reported male patients from four families (one with clinical OFDI; one with *SGBS2* and an *OFDI* mutation; two with *JBTS10* and *OFDI* mutations), would belong to a single syndrome spectrum caused by truncating *OFDI* mutations, presenting with craniofacial features (macrocephaly, depressed or broad nasal bridge, and lip abnormalities), postaxial polydactyly, respiratory insufficiency with recurrent respiratory tract infections in survivors, severe mental or developmental retardation, and brain malformations (hypoplasia or agenesis of corpus callosum and/or cerebellar vermis and posterior fossa abnormalities).

Acknowledgements

The authors are grateful to the family for their participation in this study. The authors are also thankful to Prof Germana Meroni (Cluster in Biomedicine, Trieste) for mutation analysis of *MIDI*, Dr Takeshi Futatani (Department of Pediatrics, Toyama Prefectural Central Hospital, Toyama, Japan), Dr Masahiko Kawabata (Department of Internal Medicine, Toyama Prefectural Central Hospital, Toyama, Japan), and Dr Akio Uchiyama (Department of Pathology, Toyama Prefectural Central Hospital, Toyama, Japan) for collecting clinical information; Dr Gen Nishimura (Department of Radiology, Tokyo Metropolitan Children's Medical Center) for helping radiological assessment; and Miss Junko Kunimi (Department of Medical Genetics, Shinshu University School of Medicine, Matsumoto, Japan) and Dr Shin-ya Nishio (Department of Otolaryngology, Shinshu University School of Medicine, Matsumoto,

Japan) for their technical assistance. This work was supported by research grants from the Ministry of Health, Labour and Welfare (T. K., Y. F., H. S., N. Mi., and N. Ma.), the Japan Science and Technology Agency (N. Ma.), the Strategic Research Program for Brain Sciences (N. Ma.) and a Grant-in-Aid for Scientific Research on Innovative Areas (Foundation of Synapse and Neuro-circuit Pathology) from the Ministry of Education, Culture, Sports, Science and Technology of Japan (N. Ma.), a Grant-in-Aid for Scientific Research from Japan Society for the Promotion of Science (N. Ma.), a Grant-in-Aid for Young Scientist from Japan Society for the Promotion of Science (H. S. and N. Mi.) and a grant from the Takeda Science Foundation (N. Mi. and N. Ma.). This work was performed at the Advanced Medical Research Center, Yokohama City University, Japan.

Y. T., H. D., H. S., and N. Mi. performed the genetic analysis; T. K., K. H., Y. N., K. W., and Y. F. evaluated clinical aspects of the family, recruited samples, and prepared them for the analysis. Y. T., T. K. and N. Ma. wrote the manuscript.

Ethics approval

The work was approved by the Yokohama City University (Faculty of Medicine) and the Shinshu University (School of Medicine). Patient consent was obtained.

References

1. Papillon-Leage M, Psaume J. Une malformation hereditaire de la muqueuse buccale: brides et freins anomaux. *Rev Stomatol* 1954; 55: 209–227.
2. Gorlin RJ, Psaume J. Orofaciodigital dysostosis: a new syndrome. A study of 22 cases. *J Pediatr* 1962; 61: 520–530.
3. Ferrante MI, Giorgio G, Feather SA et al. Identification of the gene for oral-facial-digital type I syndrome. *Am J Hum Genet* 2001; 68: 569–576.
4. Macca M, Franco B. The molecular basis of oral-facial-digital syndrome, type 1. *Am J Med Genet C* 2009; 151C: 318–325.
5. Toriello HV, Franco B. Oral-facial-digital syndrome type I. In: Pagon RA, Bird TD, Dolan CR, Stephens K, Adam MP, eds. *GeneReviews at genetests: Medical Genetics Information Resource* (database online). Seattle, WA: Copyright, University of Washington, 1993–2011, from <http://www.genetests.org>. Accessed on July 23, 2011.
6. Morleo M, Franco B. Dosage compensation of the mammalian X-chromosome influences the phenotypic variability of X-linked dominant male-lethal disorders. *J Med Genet* 2008; 45: 401–408.
7. Goodship J, Platt J, Smith R, Burn J. A male with type I orofacioidigital syndrome. *J Med Genet* 1991; 28: 691–694.
8. Fontanella B, Russolillo G, Meroni G. *MIDI* mutations in patients with X-linked Opitz G/BBB syndrome. *Hum Mutat* 2008; 29: 584–594.
9. Nishimura-Tadaki A, Wada T, Bano G et al. Breakpoint determination of X;autosome balanced translocations in four patients with premature ovarian failure. *J Hum Genet* 2011; 56: 156–160.
10. Budny B, Chen W, Omran H et al. A novel X-linked recessive mental retardation syndrome comprising macrocephaly and ciliary dysfunction is allelic to oral-facial-digital type I syndrome. *Hum Genet* 2006; 120: 171–178.
11. Terespolsky D, Farrell SA, Siegel-Bartelt J, Weksberg R. Infantile lethal variant of Simpson-Golabi-Behmel syndrome associated with hydrops fetalis. *Am J Med Genet* 1995; 59: 329–333.
12. Brzustowicz LM, Farrell S, Khan MB, Weksberg R. Mapping of a new *SGBS* locus to chromosome Xp22 in a family with a severe form of Simpson-Golabi-Behmel syndrome. *Am J Hum Genet* 1999; 65: 779–783.
13. Coene KL, Roepman R, Doherty D et al. *OFDI* is mutated in X-linked Joubert syndrome and interacts with *LCA5*-encoded lebercilin. *Am J Hum Genet* 2009; 85: 465–481.
14. McGraw P. The molar tooth sign. *Radiology* 2002; 229: 671–672.
15. Chance PF, Cavalier L, Satran D, Pellegrino JE, Koenig M, Dobyns WB. Clinical nosologic and genetic aspects of Joubert and related syndromes. *J Child Neurol* 1999; 14: 660–666.

Tsurusaki et al.

16. Sartori S, Ludwig K, Fortuna M et al. Dandy-Walker malformation masking the molar tooth sign: an illustrative case with magnetic resonance imaging follow-up. *J Child Neurol* 2010; 25: 1419–1422.
17. Barkovich AJ. Anomalies with cerebellar dysgenesis: vermian dysgenesis. In: Barkovich AJ, ed. *Pediatric neuroimaging*, 4th edn. Lippincott Williams & Wilkins, Philadelphia 2005: 391–396.
18. Brancati F, Dallapiccola B, Valente EM. Joubert syndrome and related disorders. *Orphanet J Rare Dis* 2010; 5: 20.
19. Prattichizzo C, Macca M, Novelli V et al. Mutational spectrum of the oral-facial-digital type I syndrome: a study on a large collection of patients. *Hum Mutat* 2008; 29: 1237–1246.
20. Thauvin-Robinet C, Cossée M, Cormier-Daire V et al. Clinical, molecular, and genotype-phenotype correlation studies from 25 cases of oral-facial-digital syndrome type 1: a French and Belgian collaborative study. *J Med Genet* 2006; 43: 54–61.
21. Thauvin-Robinet C, Franco B, Saugier-Verber P et al. Genomic deletions of *OFDI* account for 23% of oral-facial-digital type 1 syndrome after negative DNA sequencing. *Hum Mutat* 2008; 30: E320–E329.
22. Shendure J, Ji H. Next-generation DNA sequencing. *Nat Biotechnol* 2008; 26: 1135–1145.
23. Bamshad MJ, Ng SB, Bigham AW et al. Exome sequencing as a tool for Mendelian disease gene discovery. *Nat Rev Genet* 2011; 12: 745–755.
24. Tsurusaki Y, Osaka H, Hamanoue H et al. Rapid detection of a mutation causing X-linked leukodystrophy by exome sequencing. *J Med Genet* 2011; 48: 606–609.
25. Tsurusaki Y, Okamoto N, Suzuki Y et al. Exome sequencing of two patients in a family with atypical X-linked leukodystrophy. *Clin Genet* 2011; 80: 161–166.

SHORT COMMUNICATION

The diagnostic utility of exome sequencing in Joubert syndrome and related disorders

Yoshinori Tsurusaki¹, Yasuko Kobayashi², Masataka Hisano³, Shuichi Ito⁴, Hiroshi Doi¹, Mitsuko Nakashima¹, Hirotomo Saito¹, Naomichi Matsumoto¹ and Noriko Miyake¹

Joubert syndrome (JS) and related disorders (JSRD) are autosomal recessive and X-linked disorders characterized by hypoplasia of the cerebellar vermis with a characteristic ‘molar tooth sign’ on brain imaging and accompanying neurological symptoms including episodic hypernoea, abnormal eye movements, ataxia and intellectual disability. JSRD are clinically and genetically heterogeneous, and, to date, a total of 17 causative genes are known. We applied whole-exome sequencing (WES) to five JSRD families and found mutations in all: either *CEP290*, *TMEM67* or *INPP5E* was mutated. Compared with conventional Sanger sequencing, WES appears to be advantageous with regard to speed and cost, supporting its potential utility in molecular diagnosis.

Journal of Human Genetics (2013) 58, 113–115; doi:10.1038/jhg.2012.117; published online 4 October 2012

Keywords: *CEP290*; exome sequencing; *INPP5E*; Joubert syndrome; molecular diagnosis; *TMEM67*

Joubert syndrome (JS) and related disorders (JSRD) are autosomal recessive and X-linked disorders characterized by hypoplasia of the cerebellar vermis with the characteristic neuroradiological ‘molar tooth sign’ and accompanying neurological symptoms including dysregulation of breathing pattern, ataxia and developmental delay. JSRD are classified into six subtypes: pure JS, JS with ocular defect, JS with renal defect, JS with oculorenal defects, JS with hepatic defect and JS with orofaciocaudal defects.¹ To date, 17 causative genes have been identified in JSRD: *INPP5E*,² *TMEM216*,³ *AHI1*,⁴ *NPHP1*,⁵ *CEP290*,⁶ *TMEM67*,⁷ *RPGRIP1L*,⁸ *ARL13B*,⁹ *CC2D2A*,¹⁰ *OFD1*,¹¹ *TTC21B*,¹² *KIF7*,¹³ *TCTN1*,¹⁴ *TMEM237*,¹⁵ *CEP41*,¹⁶ *TMEM138*,¹⁷ and *C5ORF42*.¹⁸ Because of the clinical and genetic heterogeneity in JSRD, it can be very difficult to identify the causative mutations in individual cases.

We encountered five non-consanguineous Japanese families with JSRD (Figure 1a) and molar tooth sign was observed in all patients (Figures 1b–e, Supplementary Table 1). Peripheral blood samples were obtained from patients and their family members after written informed consent was given. To identify causative mutations, we performed whole-exome sequencing (WES) in five probands of the five families (one proband from each family). DNA was processed using the SureSelectXT Human All Exon 50 Mb library or V4 (51 Mb) library (Agilent Technologies, Santa Clara, CA, USA), and sequenced on a Genome Analyzer Iix sequencer (Illumina, San Diego, CA, USA) with 108 bp paired-end reads, or on a HiSeq2000 sequencer (Illumina) with 101 bp paired-end reads and 7 bp index reads.

Image analysis and base calling were performed by Illumina pipeline. Approximately 3.8–6.0 Gb of sequence data were mapped to the human reference genome (GRCh37.1/hg19) with Novoalign or Burrows-Wheeler Aligner. The mean depth of coverage was 55–125 reads, with 88–96% of all coding exons being covered by 5 × or more reads.

Out of all variants within exons and ±20-bp intronic regions from the exon–intron boundaries, those registered in dbSNP135, 1000 Genomes and ESP5400 and located within the segmental duplications were removed. Homozygous or compound heterozygous variants of 17 JSRD causative genes were then picked up. In patients 1, 2, 3 and 4 whose DNA was captured by the SureSelectXT Human All Exon 50 Mb library, ~90% of the entire coding regions in 13 of 17 causative genes were covered by 5 × reads or more. In patient 5 captured by the V4 (51 Mb) library, >90% of the coding region was covered by 5 × reads or more (Supplementary Table 2), indicating that the V4 library offered superior coverage to the SureSelectXT library around the regions of the JSRD genes.

All patients from the five families possessed novel compound heterozygous mutations or a homozygous mutation in known genes later confirmed by Sanger sequencing (Figure 1a): c.1862G>A (p.R621Q)/c.700dupC (p.L234Pfs*56) in *INPP5E* (9q34.3) for family 1; c.5788A>T (p.K1930*)/c.6012-12A>T in *CEP290* (12q21.32) for family 2; c.329A>G (p.D110G)/c.2322 + 5delG in *TMEM67* (8q22.1) for family 3; homozygous c.6012-12A>T in *CEP290* for family 4; and c.214G>T (p.E72*)/c.6012-12A>T in *CEP290* for family 5. No other variants within 17 known genes have been identified after excluding

¹Department of Human Genetics, Yokohama City University Graduate School of Medicine, Yokohama, Japan; ²Department of Pediatrics, Gunma University Graduate School of Medicine, Maebashi, Japan; ³Department of Nephrology, Chiba Children's Hospital, Chiba, Japan and ⁴National Center for Child Health and Development, Tokyo, Japan
Correspondence: Dr N Miyake, Department of Human Genetics, Yokohama City University Graduate School of Medicine, 3-9 Fukuura, Kanazawa-ku, Yokohama 236-0004, Japan.

E-mail: nmiyake@yokohama-cu.ac.jp

Received 31 July 2012; revised 3 September 2012; accepted 5 September 2012; published online 4 October 2012

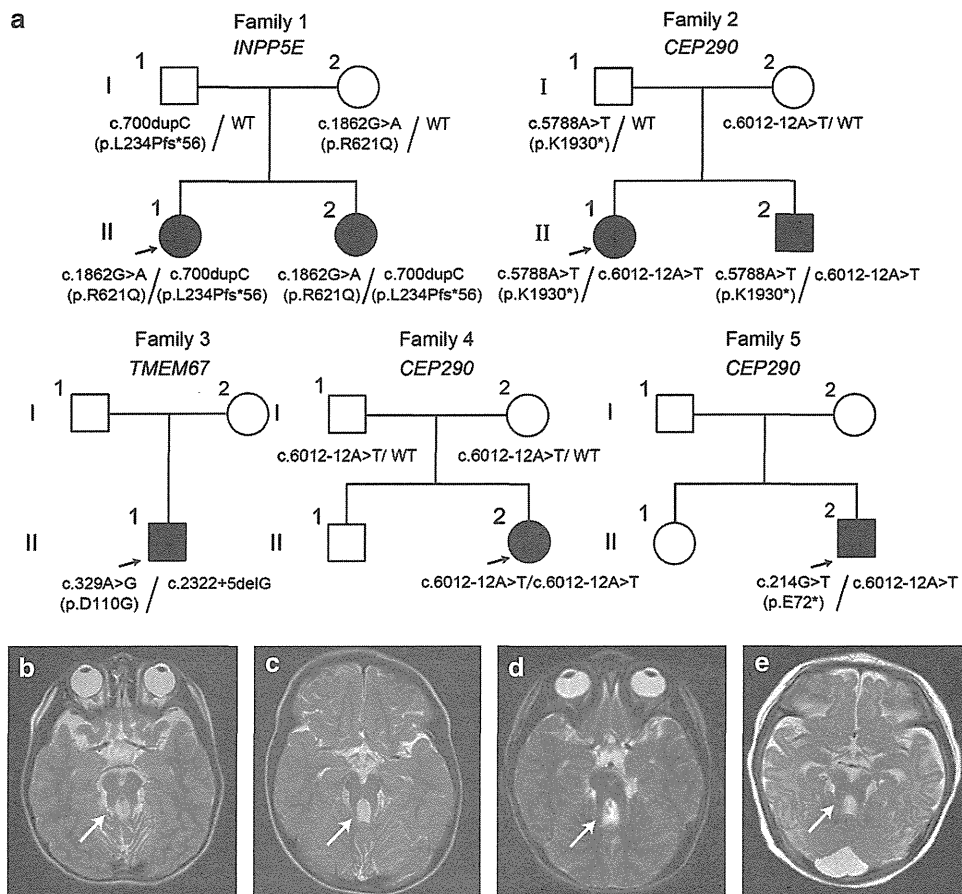


Figure 1 Familial pedigree and brain MRI of the patients. (a) JSRD families and mutations. (b) T2-weighted axial images of III-1, family 1. (c) T2-weighted axial images of III-2, family 1. (d) T2-weighted axial images of III-1, family 2. (e) T2-weighted axial images of III-2, family 2. The molar tooth sign is visible in all patients (arrowheads).

the variants of dbSNP135, 1000 Genomes and ESP5400. Clinical phenotypes caused by respective mutated genes are discussed in Supplementary text. In families 1, 2 and 4 in which parental samples were available, all parents were heterozygous carriers of one of the mutations. As parental samples were unavailable from families 3 and 5, we determined whether two mutations resided on different alleles by cloning an reverse transcriptase-PCR (RT-PCR) product amplified from total RNA of lymphoblastoid cells into a pCR4-TOPO vector (Life Technologies, Carlsbad, CA, USA) and sequencing. Each mutation was found in a different allele for both families (data not shown). Another variant, c.1894A>G (p.K632E) in *CEP290*, of family 2 was not found to be pathogenic based on web-based analyses such as SIFT, PolyPhen-2 and Mutation Taster (Supplementary Table 3). In families 2, 4 and 5 with a *CEP290* abnormality, c.6012-12A>T was shared. On the basis of our in-house 135 exome data, the allele frequency of the mutation was 1/270 allele (0.74%), indicating that it may be a rare variant in Japanese. The other mutations were not found in our in-house 135 exome data.

Splicing effects were examined in families 3 and 4. RT-PCR was performed on RNA from lymphoblastoid cells of family members using primers spanning exons 42/43 and 45/46 in family 4 and exons 20/21 and 24/25 in family 3 (sequence information available on request). In family 4, only an aberrant cDNA was detected in II-2, whereas the parents (I-1 and I-2) showed two different products including one wild-type, which was detected in a control

(Supplementary Figures 1a, b). Sequencing of the mutant product revealed a 57-bp insertion corresponding to the 3'-side of intron 43. As a result, a premature stop codon was introduced at intron 43. In family 3, RT-PCR detected a mutant cDNA in II-1 together with a wild-type product, which was detected in a control. Sequencing of the mutant product confirmed the skipping of exon 22, resulting in an in-frame 27 amino-acid deletion (Supplementary Figures 1c, d).

WES has proved a powerful tool for the identification of novel genes in genetic diseases. It also has tremendous potential for clinical diagnosis and is now being applied in the molecular diagnosis of single-gene disorders such as neurofibromatosis type 1, Marfan syndrome and multi-gene disorders such as retinitis pigmentosa.¹⁹ As shown here, WES would also be suitable for the diagnosis of JSRD, another multi-gene disorder. Though the read-coverage of the old version of SureSelect did not sufficiently collect genomic DNAs for four genes (*INPP5E*, *TMEM216*, *KIF7* and *TCTN1*), the performance of the V4 (51 Mb) library was satisfactory for all genes. Further, as exome capture technology is based on hybridization it can be refractory to homologous regions, so other methods such as multiplex PCR amplification and multiple microdroplet PCR technology could be useful in addition.

In conclusion, we were able to identify causative mutations in five non-consanguineous families with JSRD using WES. The diagnostic utility of WES is obvious, implying that WES or other next-generation sequencing technologies will be a main factor of molecular diagnosis.

ACKNOWLEDGEMENTS

We thank the patients and their families for their participation in this study. This work was supported by research grants from the Ministry of Health, Labor and Welfare (HS, N Matsumoto, N Miyake), the Japan Science and Technology Agency (N Matsumoto), the Strategic Research Program for Brain Sciences (N Matsumoto) and a Grant-in-Aid for Scientific Research on Innovative Areas-(Transcription cycle)-from the Ministry of Education, Culture, Sports, Science and Technology of Japan (N Matsumoto), a Grant-in-Aid for Scientific Research from Japan Society for the Promotion of Science (N Matsumoto), a Grant-in-Aid for Young Scientist from Japan Society for the Promotion of Science (HS, N Miyake) and a grant from the Takeda Science Foundation (N Matsumoto, N Miyake).

Web Resources: The URLs for data presented herein are as follows: Novoalign, <http://www.novocraft.com/main/index.php>; Burrows-Wheeler Aligner, <http://bio-bwa.sourceforge.net/>; SIFT, <http://sift.jcvi.org/>; PolyPhen-2, <http://genetics.bwh.harvard.edu/pph2/>; Mutation Taster, <http://neurocore.charite.de/MutationTaster/>

- 1 Brancati, F., Dallapiccola, B. & Valente, E. M. Joubert Syndrome and related disorders. *Orphanet. J. Rare Dis.* **5**, 20 (2010).
- 2 Bielas, S. L., Silhavy, J. L., Brancati, F., Kisseleva, M. V., Al-Gazali, L., Sztriha, L. *et al.* Mutations in INPP5E, encoding inositol polyphosphate-5-phosphatase E, link phosphatidylinositol signaling to the ciliopathies. *Nat. Genet.* **41**, 1032–1036 (2009).
- 3 Valente, E. M., Logan, C. V., Mougou-Zerelli, S., Lee, J. H., Silhavy, J. L., Brancati, F. *et al.* Mutations in TMEM216 perturb ciliogenesis and cause Joubert, Meckel and related syndromes. *Nat. Genet.* **42**, 619–625 (2010).
- 4 Ferland, R. J., Eyaid, W., Collura, R. V., Tully, L. D., Hill, R. S., Al-Nouri, D. *et al.* Abnormal cerebellar development and axonal decussation due to mutations in AHI1 in Joubert syndrome. *Nat. Genet.* **36**, 1008–1013 (2004).
- 5 Parisi, M. A., Bennett, C. L., Eckert, M. L., Dobyns, W. B., Gleeson, J. G., Shaw, D. W. *et al.* The NPHP1 gene deletion associated with juvenile nephronophthisis is present in a subset of individuals with Joubert syndrome. *Am. J. Hum. Genet.* **75**, 82–91 (2004).
- 6 Valente, E. M., Silhavy, J. L., Brancati, F., Barrano, G., Krishnaswami, S. R., Castori, M. *et al.* Mutations in CEP290, which encodes a centrosomal protein, cause pleiotropic forms of Joubert syndrome. *Nat. Genet.* **38**, 623–625 (2006).

- 7 Baala, L., Romano, S., Khaddour, R., Saunier, S., Smith, U. M., Audollent, S. *et al.* The Meckel-Gruber syndrome gene, MKS3, is mutated in Joubert syndrome. *Am. J. Hum. Genet.* **80**, 186–194 (2007).
- 8 Arts, H. H., Doherty, D., van Beersum, S. E., Parisi, M. A., Letteboer, S. J., Gorden, N. T. *et al.* Mutations in the gene encoding the basal body protein RPGRI1, a nephrocystin-4 interactor, cause Joubert syndrome. *Nat. Genet.* **39**, 882–888 (2007).
- 9 Cantagrel, V., Silhavy, J. L., Bielas, S. L., Swistun, D., Marsh, S. E., Bertrand, J. Y. *et al.* Mutations in the cilia gene ARL13B lead to the classical form of Joubert syndrome. *Am. J. Hum. Genet.* **83**, 170–179 (2008).
- 10 Gorden, N. T., Arts, H. H., Parisi, M. A., Coene, K. L., Letteboer, S. J., van Beersum, S. E. *et al.* CC2D2A is mutated in Joubert syndrome and interacts with the ciliopathy-associated basal body protein CEP290. *Am. J. Hum. Genet.* **83**, 559–571 (2008).
- 11 Coene, K. L., Roepman, R., Doherty, D., Afroze, B., Kroes, H. Y., Letteboer, S. J. *et al.* OFD1 is mutated in X-linked Joubert syndrome and interacts with LCA5-encoded lebercilin. *Am. J. Hum. Genet.* **85**, 465–481 (2009).
- 12 Davis, E. E., Zhang, Q., Liu, Q., Diplas, B. H., Davey, L. M., Hartley, J. *et al.* TTC21B contributes both causal and modifying alleles across the ciliopathy spectrum. *Nat. Genet.* **43**, 189–196 (2011).
- 13 Dafinger, C., Liebau, M. C., Elsayed, S. M., Hellenbroich, Y., Boltshauser, E., Korenke, G. C. *et al.* Mutations in KIF7 link Joubert syndrome with Sonic Hedgehog signaling and microtubule dynamics. *J. Clin. Invest.* **121**, 2662–2667 (2011).
- 14 Garcia-Gonzalo, F. R., Corbit, K. C., Sirerol-Piquer, M. S., Ramaswami, G., Otto, E. A., Noriega, T. R. *et al.* A transition zone complex regulates mammalian ciliogenesis and ciliary membrane composition. *Nat. Genet.* **43**, 776–784 (2011).
- 15 Huang, L., Szymanska, K., Jensen, V. L., Janecke, A. R., Innes, A. M., Davis, E. E. *et al.* TMEM237 is mutated in individuals with a Joubert syndrome related disorder and expands the role of the TMEM family at the ciliary transition zone. *Am. J. Hum. Genet.* **89**, 713–730 (2011).
- 16 Lee, J. E., Silhavy, J. L., Zaki, M. S., Schroth, J., Bielas, S. L., Marsh, S. E. *et al.* CEP41 is mutated in Joubert syndrome and is required for tubulin glutamylation at the cilium. *Nat. Genet.* **44**, 193–199 (2012).
- 17 Lee, J. H., Silhavy, J. L., Lee, J. E., Al-Gazali, L., Thomas, S., Davis, E. E. *et al.* Evolutionarily assembled cis-regulatory module at a human ciliopathy locus. *Science* **335**, 966–969 (2012).
- 18 Srour, M., Schwartzentruber, J., Hamdan, F. F., Ospina, L. H., Patry, L., Labuda, D. *et al.* Mutations in C5ORF42 Cause Joubert Syndrome in the French Canadian Population. *Am. J. Hum. Genet.* **90**, 693–700 (2012).
- 19 Zhang, W., Cui, H. & Wong, L. J. Application of next generation sequencing to molecular diagnosis of inherited diseases. *Top. Curr. Chem.* (e-pub ahead of print 11 May 2012; doi:10.1007/128_2012_325).

Supplementary Information accompanies the paper on Journal of Human Genetics website (<http://www.nature.com/jhg>)

A *DYNC1H1* mutation causes a dominant spinal muscular atrophy with lower extremity predominance

Yoshinori Tsurusaki · Shinji Saitoh ·
Kazuhiro Tomizawa · Akira Sudo · Naoko Asahina ·
Hideaki Shiraishi · Jun-ichi Ito · Hajime Tanaka ·
Hiroshi Doi · Hirotomo Saito · Noriko Miyake ·
Naomichi Matsumoto

Received: 24 February 2012 / Accepted: 3 July 2012
© Springer-Verlag 2012

Abstract Whole-exome sequencing of two affected sibs and their mother who showed a unique quadriceps-dominant form of neurogenic muscular atrophy disclosed a heterozygous *DYNC1H1* mutation [p.H306R (c.917A>G)]. The identical mutation was recently reported in a pedigree with the axonal form of Charcot–Marie–Tooth disease. Three other missense mutations in *DYNC1H1* were also identified in families with dominant spinal muscular atrophy with lower extremity predominance. Their clinical features were consistent with those of our family. Our study has demonstrated that the same *DYNC1H1* mutation could cause spinal muscular atrophy as well as distal neuropathy, indicating pleiotropic effects of the mutation.

Keywords Spinal muscular atrophy with lower extremity predominance · *DYNC1H1* · Whole-exome sequencing · Charcot–Marie–Tooth disease · Allelic disease

Introduction

DYNC1H1 encodes cytoplasmic dynein heavy chain 1, which is a subunit of the primary motor protein responsible for retrograde axonal transport in neurons [1]. Weedon et al. first identified a missense mutation [p.H306R (c.917A>G)] of *DYNC1H1* in a large family with axonal Charcot–Marie–Tooth (CMT) disease by using exome sequencing, indicating the significance of *DYNC1H1* in the peripheral nerve axon [2]. Subsequently, Harms et al. reported three other missense mutations in the tail domain of *DYNC1H1* in families with dominant spinal muscular atrophy with lower extremity predominance (SMA-LED, OMIM 158600), expanding the role of *DYNC1H1* to maintenance of motor neuron itself [3]. Recently, two de novo missense mutations have also been identified in patients with severe intellectual disability and variable neuronal migration defects [4].

Authorship Y.T. and S.S. contributed equally to this work.

Y. Tsurusaki · H. Doi · H. Saito · N. Miyake · N. Matsumoto (✉)
Department of Human Genetics, Yokohama City University
Graduate School of Medicine,
3-9 Fukuura, Kanazawa-ku,
Yokohama 236-0004, Japan
e-mail: naomat@yokohama-cu.ac.jp

S. Saitoh (✉)
Department of Pediatrics and Neonatology, Graduate School
of Medical Sciences, Nagoya City University,
Kawasumi-1, Mizuho-cho, Mizuho-ku,
Nagoya 467-8601, Japan
e-mail: ss11@med.nagoya-cu.ac.jp

K. Tomizawa
Department of Pediatrics, Nakashibetsu Town Hospital,
Nakashibetsu, Japan

A. Sudo
Department of Pediatrics, Sapporo City General Hospital,
Sapporo, Japan

N. Asahina · H. Shiraishi
Department of Pediatrics, Hokkaido University Graduate School
of Medicine,
Sapporo, Japan

J.-i. Ito
Department of Pediatrics, Taiyo no Sono,
Date, Japan

H. Tanaka
Department of Pediatrics, Asahikawa Habilitation Center
for Disabled Children,
Asahikawa, Japan

Therefore, *DNYCIH1* may have broad biological effects on development and maintenance of the nervous system.

In this study, we describe a family containing three individuals with dominant spinal muscular atrophy with lower extremity predominance. Exome sequencing identified an identical *DNYCIH1* mutation found in a pedigree with axonal CMT [2], demonstrating the pleiotropic effects of the *DNYCIH1* mutation.

Subjects and methods

Subjects

Patient 1 This female patient was born after 41 weeks of gestation. Pregnancy was uneventful. Birth weight was 3,080 g. Her initial development was normal, and head control was recognized at 3–4 months. Late infantile motor development was mildly delayed, and she could walk unassisted at 1 year and 8 months. Unstable gait persisted thereafter, and she was referred to us at 3 years and 1 month of age for evaluation. On examination, proximal lower limb-dominant muscle atrophy and decreased deep tendon reflex were noted. Gower's sign was positive. No other neurological deficits were demonstrated. No sensory disturbance or ataxia was present.

The following examinations were performed at 3 years and 1 month of age. Neither serum transaminase nor creatine kinase was elevated. Motor nerve conduction velocity was within the normal limits (55.8 m/s for the right tibial nerve). Brain MRI revealed normal findings. Muscle computed tomography (CT) demonstrated severe atrophy and lipid degeneration, predominantly in the bilateral quadriceps femoris muscle (Fig. 1). The upper limbs and distal lower limbs were not affected. A muscle biopsy from the quadriceps femoris muscle demonstrated severe grouping atrophy of type 2 fibers with a massive increase in the amount of fibrous tissue and sparse enlarged type 1 fibers (Fig. 2).

The patient is currently 18 years old and graduated from regular high school. Her motor development has steadily progressed, and she only shows moderate proximal lower limb-dominant muscle weakness and atrophy. She can walk unassisted and shows a waddling gait and positive Gower's sign. No sensory disturbance or ataxia is noted. She does not have any intellectual disability.

Patient 2 Patient 2 is the half brother of patient 1. He was born after 38 weeks of gestation to the same mother and a different father from patient 1's. His birth weight was 2,405 g. He could control his head at 3–4 months, turn over at 6 months, and sit unassisted at 7–8 months. His motor development was delayed thereafter, and he walked unassisted at 1 year and 7 months. His mental development was

normal. Because of a persistently unstable gait, he was hospitalized and examined at 5 years and 11 months. Physical examination revealed moderate muscle weakness in the proximal lower limb, but Gower's sign was negative. Deep tendon reflex was normal. No sensory disturbance or ataxia was recognized. Ankle joint contracture and foot deformity were absent.

The following examinations were performed at 5 years and 11 months of age. Serum transaminase and creatine kinase levels were normal. Brain and spinal MRI revealed no abnormal findings. Motor nerve conduction velocity and amplitude were within the normal limits (51.1 m/s, 4.6 mV for the right median nerve, 51.1 m/s, 9.9 mV for the right tibial nerve). Sensory nerve conduction velocity and amplitude were also within the normal limits (57.3 m/s, 28.4 μ V for the right median nerve, 63.7 m/s, 9.6 μ V for the right sural nerve). Needle electromyography of the anterior tibial muscle showed long high-amplitude discharges (3.5–4.0 mV, 10 ms) consistent with a neurogenic pattern, although no denervation potential, including positive sharp wave or fibrillation potential, was present, while the right biceps brachii showed inconclusive results. Muscle CT revealed severe atrophy and lipid degeneration, most predominantly in the bilateral quadriceps femoris. The upper limbs and distal lower limbs were not affected (Fig. 1).

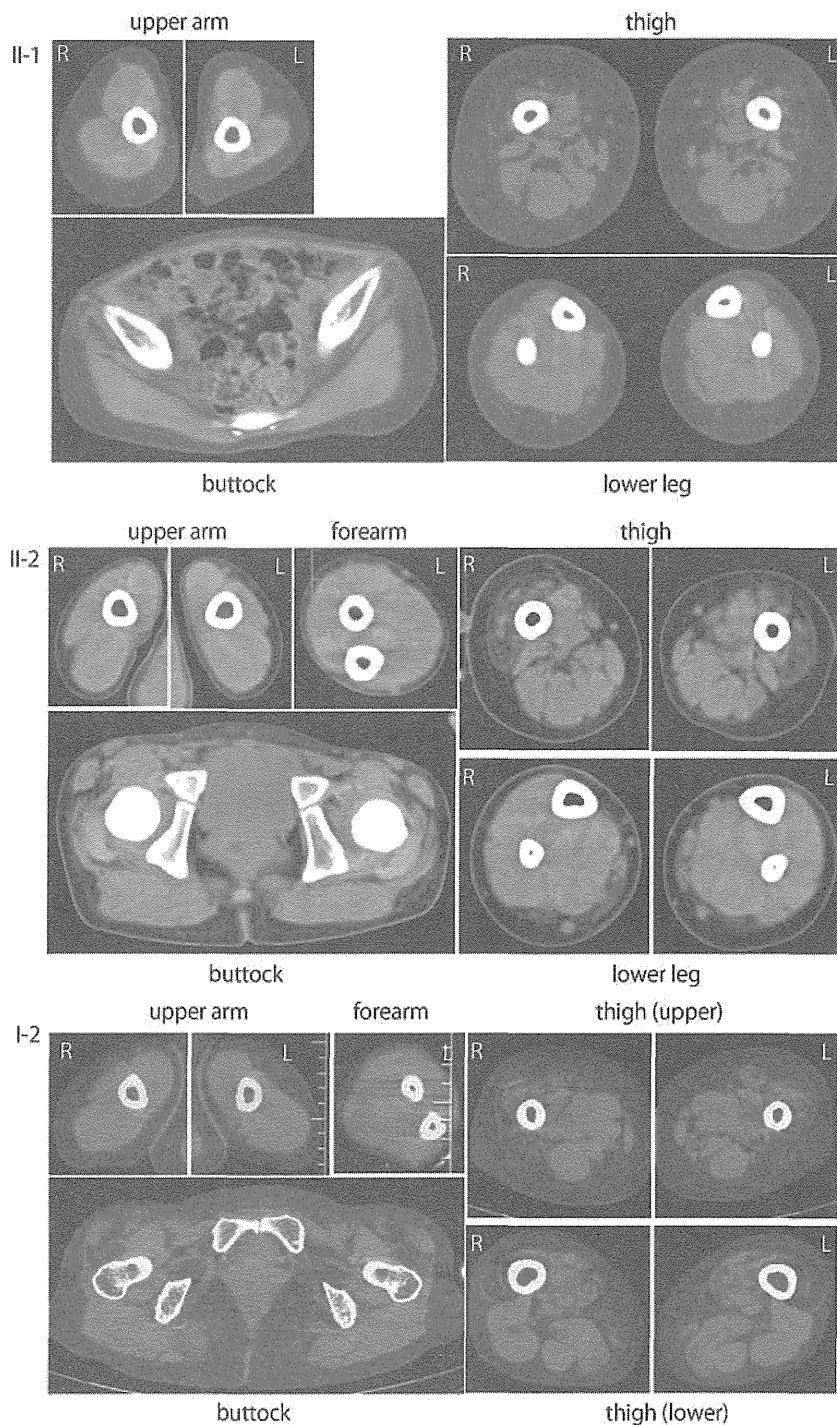
The patient is now 12 years old and can walk unassisted but with a waddling gait. He has shown no further deterioration of motor function. Proximal lower limb weakness and wasting are evident, but the patient shows no upper limb weakness. No sensory disturbance or ataxia has been recognized.

Patient 3 Patient 3 is the mother of the two sibs. She is currently 50 years of age. No family history (except for her children) of neuromuscular disorders was noted. Until we examined the second sib, she had not been noted to have proximal lower limb muscle weakness. She did not recall her infantile development, and it was impossible to obtain further information. She graduated from a regular high school, married, and raised her children. She has not shown any neurological deterioration. She did not show a waddling gait, but had difficulty squatting. She was examined at 44 years of age. Her deep tendon reflex was normal, and no ankle joint contracture was present. Muscle CT revealed bilateral quadriceps-dominant muscle atrophy and lipid degeneration (Fig. 1). She also demonstrated mild muscle atrophy in her hip. Unfortunately, CT of the distal lower limb muscle could not be performed.

Exome sequencing

We performed the whole-exome sequencing of two patients (II-1 and II-2; Fig. 3a). Three micrograms of genomic DNA

Fig. 1 Muscle imaging. Muscle computed tomography images of patient II-1 at the age of 3 years and 1 month (*upper*), patient II-2 at the age of 5 years and 11 months (*middle*), and patient I-1 at the age of 44 years (*lower*) are displayed. *R* right, *L* left



was processed using a SureSelect Human All Exon Kit v.1 (approximately 180,000 exons covering 38 Mb of the CCDS database) (Agilent Technologies, Santa Clara, CA) according to the manufacturer's protocol. Captured DNA was diluted to a concentration of 8 pM and sequenced on a Genome Analyzer IIx (Illumina, San Diego, CA) with 76-bp paired-end reads. We used two of the eight lanes in the flow cell (Illumina). Image analyses and base calling were

performed by sequence control software real-time analysis and/or Off-line Basecaller software v1.6.0 (Illumina). Alignment was performed using CASAVA software v1.6.0. The quality-controlled (Path Filter) reads were mapped to the human reference genome (UCSC hg19, NCBI build 37), using mapping and assembly with quality (MAQ) and NextGENe software v2.0 (SoftGenetics, State College, PA). SNPs in MAQ-passed reads were annotated using the

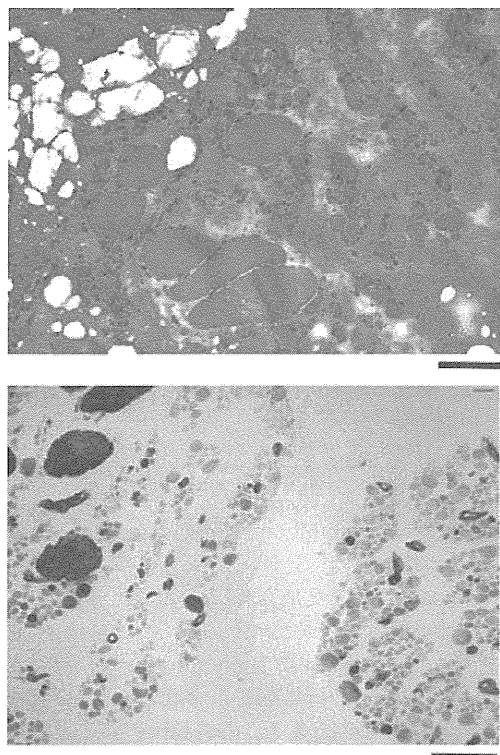
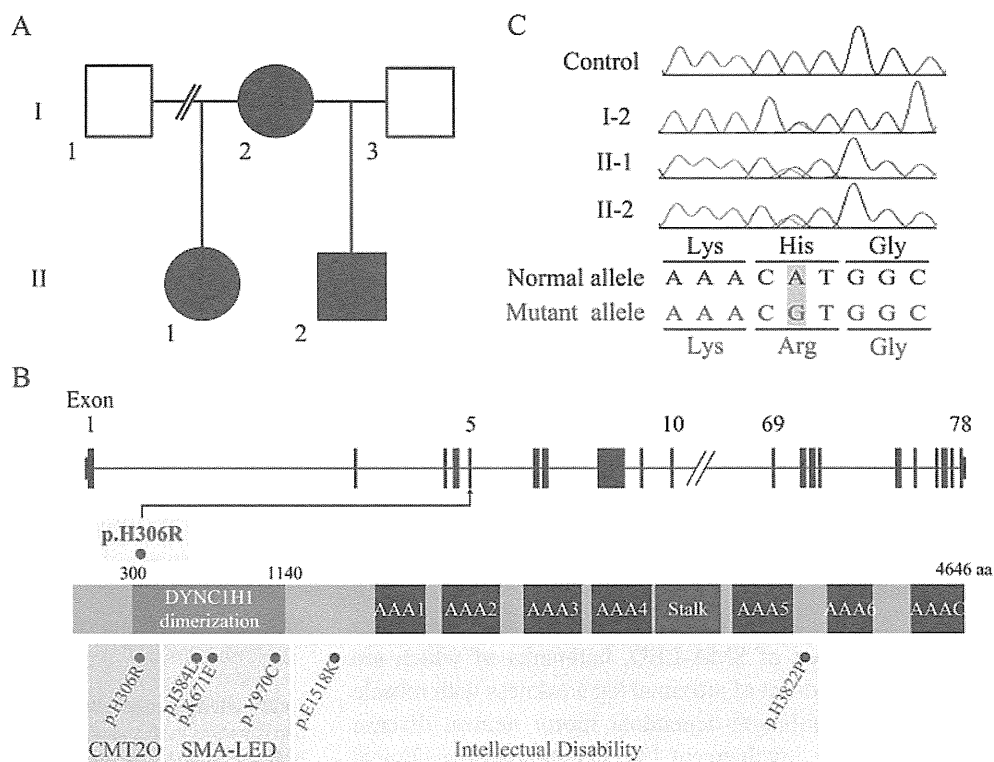


Fig. 2 Histological study. Hematoxylin–eosin staining (*upper*) and ATPase staining (pH=4.6, *lower*) of the quadriceps femoris muscle of patient II-1. The scale bar indicates 100 μ m in length

SeattleSeq Annotation website (<http://gvs.gs.washington.edu/SeattleSeqAnnotation/>).

Fig. 3 Genetic study. **a** Familial pedigree. **b** The gene structure of *DYNC1H1* with the mutation [p.H306R (c.917A>G)] (*upper*), the protein structure with functional domains (*middle*), and reported mutations corresponding to respective diseases (*lower*). AAA ATPase domains (AAA 1 to 6), AAAC unrelated seventh domain. **c** Sequences of a control and the family members are displayed. Heterozygous mutations are observed in patients I-2, II-1, and II-2



Priority scheme and capillary sequencing

We adopted a prioritization scheme used in recent studies to identify the pathogenic mutation [5–7]. Called variants found by each informatics method filtered into unregistered variants (excluding registered dbSNP131 and 1,000 genomes), overlapping variants called in common by NextGENe and MAQ, nonsynonymous changes (NS), splice site mutations (± 2 bp from the exon–intron junctions) (SS), small insertions or deletions (indels), and overlapping variants called in II-1 and II-2 were checked, and variants found in our 33 in-house exomes derived from 19 healthy individuals and 14 individuals with unrelated diseases were excluded (Table 1). An online human genome mutation database (HGMD, <https://portal.biobase-international.com/hgmd/pro/start.php>) was referred to as a reference for disease-causing mutations. The variants were confirmed as true positives by Sanger sequencing of polymerase chain reaction products amplified using genomic DNA as a template. Sanger sequencing was performed on an ABI3500XL or ABI3100 autosequencer (Life Technologies, Carlsbad, CA). Sequencing data were analyzed using Sequencer software (Gene Codes Corporation, Ann Arbor, MI).

A total of 177 Japanese control samples (354 alleles) were checked by high-resolution melting analysis using a LightCycler 480 (Roche Diagnostics, Otsu, Japan) to see the variant frequency. The reaction was performed in 10 μ l containing 10 ng of genomic DNA, 0.2 mM dNTPs,

Table 1 Variant priority scheme of exome sequencing data

| | Half sister | | Half brother | |
|--|--------------------------------------|------------------|--------------|------------------|
| | NextGENe | MAQ (SeattleSeq) | NextGENe | MAQ (SeattleSeq) |
| Total variants called | 73,966 | 174,757 | 73,370 | 163,707 |
| Autosomal+chr X | 71,522 | 174,165 | 70,068 | 163,013 |
| Unknown SNP variants (dbSNP, 1,000 genomes) | 11,132 | 21,284 | 10,857 | 19,858 |
| MAQs were annotated using SeattleSeq annotation. The annotation includes gene names, dbSNP rs IDs, and SNP functions (e.g., missense), protein positions and amino acid changes. <i>NS</i> nonsynonymous, <i>SS</i> splice site (± 2 bp), <i>I</i> indels | Overlap of NextGENe and MAQ | | 1,482 | |
| | NS/SS/I | | 411 | |
| | Overlapping in half sibs | | 135 | |
| | Unknown variants (in-house database) | | 62 | |

0.125 U of ExTaq (Takara Bio, Inc., Otsu, Japan), 1× buffer, and 1.5 μ M SYTO9 (Invitrogen, Carlsbad, CA).

Results

Approximately 9.8 and 9.5 Gb of sequence data were generated for II-1 and II-2, respectively. This approach resulted in more than 85.8 % (II-1) and 86.5 % (II-2) of the target regions being covered by ten reads or more. Two informatics methods identified 62 potentially pathogenic changes (Table 1). We found a missense mutation [p.H306R (c.917A>G)] in *DYNC1H1* from among 62 variants using the HGMD as a reference; this mutation has been reported as a causative mutation for CMT disease [2]. The heterozygous missense mutation was confirmed in I-2, II-1, and II-2 (Fig. 3b). This missense mutation was not found in 177 control samples.

Discussion

The identical *DYNC1H1* mutation (p.H306R) found in a large pedigree with axonal type of CMT disease was detected by exome sequencing in a family with a unique form of quadriceps-dominant neurogenic muscular atrophy [2]. Three members of the family demonstrated very similar clinical features, which were distinct from CMT disease. The most striking feature was a unique distribution of muscle involvement. The quadriceps femoris muscle was almost selectively involved in the early course of the disease, and the proximal lower limb was predominantly involved throughout the disease course. Recently, three other missense mutations were detected in families with SMA-LED. Clinical features of the current family are essentially consistent with those of SMA-LED, hallmarks of which are early childhood onset of proximal leg weakness with muscle atrophy and nonlength-dependent motor neuron disease without sensory involvement [3]. Nonprogressive clinical

course despite early childhood onset as in our family should be another hallmark of SMA-LED. These cumulative data clearly indicate that *DYNC1H1* plays an essential role in maintenance of spinal motor neurons and their axon.

Thus far, four missense mutations (p.H306R, p.I584L, p.K671E, p.Y970C) identified in human cases of CMT or SMA-LED are located in the same tail domain for *DYNC1H1* dimerization. It is of note that three missense mutations (p.F580Y, p.G1042A, p.T1057C) found in mouse models are also located in the tail domain [8–10]. These mice involve not only spinal motor neurons but also sensory and cortical neurons. The tail domain is thought to be essential for dimerization of dynein heavy chains, and thus, missense mutations in the tail domain may disrupt function of dynein complex formation in a dominant negative manner. Two distinct de novo mutations (p.E1518K, p.H3822P) identified in patients with severe intellectual disability and variable neuronal migration defects were located outside of the tail domain. These patients also showed possible peripheral nerve involvement, but formal neurophysiological investigation was not available. Since mice with *Dync1h1* abnormality show broad central nervous system involvement, *DNYCIH1* is likely to cause a wide range of neuronal migration disorders.

CMT disease with the p.H306R mutation has been designated as CMT2O (OMIM 614228). Most members of the pedigree with p.H306R reported by Weedon et al. demonstrated distal dominant muscle weakness, while one patient showed proximal lower limb-dominant muscle atrophy as in our family [2]. Therefore, the same missense mutation in the tail domain could cause CMT2O phenotype and SMA-LED phenotype even within the same pedigree. It is hard to explain the underlying mechanism of pleiotropic effects of the mutation. Further studies are absolutely necessary to elucidate phenotype–genotype correlation and pleiotropic mutational consequences.

Acknowledgments We would like to thank the family for their participation in this study. This work was supported by research grants from the Ministry of Health, Labour and Welfare (H.S., N. Miyake, and

N. Matsumoto); a Grant-in-Aid for Scientific Research from the Japan Society for the Promotion of Science (N. Miyake and N. Matsumoto); a grant from the Japan Science and Technology Agency (N. Matsumoto), the Strategic Research Program for Brain Sciences (N. Matsumoto); a Grant-in-Aid for Scientific Research on Innovative Areas (Foundation of Synapse and Neurocircuit Pathology) from the Ministry of Education, Culture, Sports, Science and Technology of Japan (N. Matsumoto); a research grant from Naito Foundation (N. Matsumoto); and research grants from Takeda Science Foundation (N. Miyake and N. Matsumoto). This work was performed at the Advanced Medical Research Center, Yokohama City University, Japan.

References

- Pfister KK, Shah PR, Hummerich H, Russ A, Cotton J, Annuar AA, King SM, Fisher EM (2006) Genetic analysis of the cytoplasmic dynein subunit families. *PLoS Genet* 2(1):e1. doi:10.1371/journal.pgen.0020001
- Weedon MN, Hastings R, Caswell R, Xie W, Paszkiewicz K, Antoniadis T, Williams M, King C, Greenhalgh L, Newbury-Ecob R, Ellard S (2011) Exome sequencing identifies a DYNC1H1 mutation in a large pedigree with dominant axonal Charcot-Marie-Tooth disease. *Am J Hum Genet* 89(2):308–312. doi:10.1016/j.ajhg.2011.07.002
- Harms MB, Ori-McKenney KM, Scoto M, Tuck EP, Bell S, Ma D, Masi S, Allred P, Al-Lozi M, Reilly MM, Miller LJ, Jani-Acsadi A, Pestronk A, Shy ME, Muntoni F, Vallee RB, Baloh RH (2012) Mutations in the tail domain of DYNC1H1 cause dominant spinal muscular atrophy. *Neurology* 78(22):1714–1720. doi:10.1212/WNL.0b013e3182556c05
- Willemsen MH, Vissers LE, Willemsen MA, van Bon BW, Kroes T, de Ligt J, de Vries BB, Schoots J, Lugtenberg D, Hamel BC, van Bokhoven H, Brunner HG, Veltman JA, Kleefstra T (2012) Mutations in DYNC1H1 cause severe intellectual disability with neuronal migration defects. *J Med Genet* 49(3):179–183. doi:10.1136/jmedgenet-2011-100542
- Tsurusaki Y, Okamoto N, Suzuki Y, Doi H, Saitsu H, Miyake N, Matsumoto N (2011) Exome sequencing of two patients in a family with atypical X-linked leukodystrophy. *Clin Genet* 80(2):161–166. doi:10.1111/j.1399-0004.2011.01721.x
- Saitsu H, Osaka H, Sasaki M, Takahashi J, Hamada K, Yamashita A, Shibayama H, Shiina M, Kondo Y, Nishiyama K, Tsurusaki Y, Miyake N, Doi H, Ogata K, Inoue K, Matsumoto N (2011) Mutations in POLR3A and POLR3B encoding RNA polymerase III subunits cause an autosomal-recessive hypomyelinating leukoencephalopathy. *Am J Hum Genet* 89(5):644–651. doi:10.1016/j.ajhg.2011.10.003
- Doi H, Yoshida K, Yasuda T, Fukuda M, Fukuda Y, Morita H, Ikeda S, Kato R, Tsurusaki Y, Miyake N, Saitsu H, Sakai H, Miyatake S, Shiina M, Nukina N, Koyano S, Tsuji S, Kuroiwa Y, Matsumoto N (2011) Exome sequencing reveals a homozygous SYT14 mutation in adult-onset, autosomal-recessive spinocerebellar ataxia with psychomotor retardation. *Am J Hum Genet* 89(2):320–327. doi:10.1016/j.ajhg.2011.07.012
- Hafezparast M, Klocke R, Ruhrberg C, Marquardt A, Ahmad-Annuar A, Bowen S, Lalli G, Witherden AS, Hummerich H, Nicholson S, Morgan PJ, Oozageer R, Priestley JV, Averill S, King VR, Ball S, Peters J, Toda T, Yamamoto A, Hiraoka Y, Augustin M, Korthaus D, Wattler S, Wabnitz P, Dickneite C, Lampel S, Boehme F, Peraus G, Popp A, Rudelius M, Schlegel J, Fuchs H, Hrabe de Angelis M, Schiavo G, Shima DT, Russ AP, Stumm G, Martin JE, Fisher EM (2003) Mutations in dynein link motor neuron degeneration to defects in retrograde transport. *Science* 300(5620):808–812. doi:10.1126/science.1083129
- Chen XJ, Levedakou EN, Millen KJ, Wollmann RL, Soliven B, Popko B (2007) Proprioceptive sensory neuropathy in mice with a mutation in the cytoplasmic dynein heavy chain 1 gene. *J Neurosci* 27(52):14515–14524. doi:10.1523/JNEUROSCI.4338-07.2007
- Ori-McKenney KM, Vallee RB (2011) Neuronal migration defects in the Loa dynein mutant mouse. *Neural Dev* 6:26. doi:10.1186/1749-8104-6-26